

NLRP3 Inflammasome Priming in the Retina of Diabetic Mice Requires REDD1-Dependent Activation of GSK3 β

Christopher M. McCurry,¹ Siddharth Sunilkumar,¹ Sandeep M. Subrahmanian,¹ Esmā I. Yerlikaya,¹ Allyson L. Toro,¹ Ashley M. VanCleave,¹ Shaunaci A. Stevens,¹ Alistair J. Barber,² Jeffery M. Sundstrom,² and Michael D. Dennis^{1,2}

¹Department of Cellular and Molecular Physiology, Penn State College of Medicine, Hershey, Pennsylvania, United States

²Department of Ophthalmology, Penn State College of Medicine, Hershey, Pennsylvania, United States

Correspondence: Michael D. Dennis, Department of Cellular and Molecular Physiology, H166, Penn State College of Medicine, 500 University Drive, Hershey PA 17033, USA; mdennis@psu.edu.

CMM and SS contributed equally to this work.

Received: September 27, 2023

Accepted: March 4, 2024

Published: March 28, 2024

Citation: McCurry CM, Sunilkumar S, Subrahmanian SM, et al. NLRP3 inflammasome priming in the retina of diabetic mice requires REDD1-dependent activation of GSK3 β . *Invest Ophthalmol Vis Sci.* 2024;65(3):34. <https://doi.org/10.1167/iovs.65.3.34>

PURPOSE. Inflammasome activation has been implicated in the development of retinal complications caused by diabetes. This study was designed to identify signaling events that promote retinal NOD-, LRR-, and pyrin domain-containing protein 3 (NLRP3) inflammasome activation in response to diabetes.

METHODS. Diabetes was induced in mice by streptozotocin administration. Retinas were examined after 16 weeks of diabetes. Human MIO-M1 Müller cells were exposed to hyperglycemic culture conditions. Genetic and pharmacological interventions were used to interrogate signaling pathways. Visual function was assessed in mice using a virtual optomotor system.

RESULTS. In the retina of diabetic mice and in Müller cell cultures, NLRP3 and interleukin-1 β (IL-1 β) were increased in response to hyperglycemic conditions and the stress response protein Regulated in Development and DNA damage 1 (REDD1) was required for the effect. REDD1 deletion prevented caspase-1 activation in Müller cells exposed to hyperglycemic conditions and reduced IL-1 β release. REDD1 promoted nuclear factor κ B signaling in cells exposed to hyperglycemic conditions, which was necessary for an increase in NLRP3. Expression of a constitutively active GSK3 β variant restored NLRP3 expression in REDD1-deficient cells exposed to hyperglycemic conditions. GSK3 activity was necessary for increased NLRP3 expression in the retina of diabetic mice and in cells exposed to hyperglycemic conditions. Müller glia-specific REDD1 deletion prevented increased retinal NLRP3 levels and deficits in contrast sensitivity in diabetic mice.

CONCLUSIONS. The data support a role for REDD1-dependent activation of GSK3 β in NLRP3 inflammasome transcriptional priming and in the production of IL-1 β by Müller glia in response to diabetes.

Keywords: diabetic retinopathy, DDIT4, RTP801, Müller glia, hyperglycemia

Diabetic retinopathy is the most common microvascular complication of diabetes and the leading cause of vision loss among working-age adults.¹ It is widely accepted that neuroinflammation contributes to the progression of retinal pathology that is caused by diabetes, but the specific molecular mechanisms that drive the immune response in the retina of diabetic patients remains poorly defined.² Evidence supports that the proinflammatory cytokine interleukin-1 β (IL-1 β) plays a key role in the retinal complications that are caused by diabetes.³ In fact, genetic or pharmacological inhibition of IL-1 β signaling prevents the development of vascular pathology in the retina of diabetic mice.⁴ IL-1 β is synthesized as a pro-IL-1 β zymogen that must undergo proteolytic cleavage by caspase-1 to generate the secreted cytokine.⁵ In turn, caspase-1 also requires proteolysis for its activation, which is controlled by large multiprotein complexes known as inflammasomes.⁶

Inflammasomes are composed of a sensor protein, a caspase, and one or more adapter proteins that assemble in response to pathogen- or damage-associated molecular patterns.⁷ Among inflammasomes, the NOD-, LRR-, and pyrin domain-containing protein 3 (NLRP3) inflammasome is best known, in part owing to its unique sensitivity to a range of stimuli that impact cellular homeostasis.⁸ NLRP3 inflammasome activity is controlled by a two-step process that involves the (1) priming and (2) activation of the NLRP3 inflammasome complex.^{9,10} Priming includes upregulation of *Nlrp3* and *Il1b* messenger RNAs (mRNAs) upon activation of the transcription factor nuclear κ B (NF- κ B) that licenses NLRP3 inflammasome activity.¹¹ NLRP3 transcriptional priming and NLRP3 inflammasome activation are seen in both preclinical models of diabetes and in patients with diabetic retinopathy.^{12–17} *Nlrp3* mRNA knockdown by an intravitreal shRNA prevents an increase in both IL-1 β protein abundance and vascular permeability in the retina of strepto-

zotocin (STZ) diabetic rats.¹³ Similar beneficial effects were also observed in the retina of diabetic rats treated intravitreally with an inhibitor that binds NLRP3 directly to prevent oligomerization.¹⁸ However, the specific signaling events that contribute to NLRP3 inflammasome activation in the context of diabetic retinopathy remain to be fully defined.

NF- κ B is a central mediator of immune function, and aberrant NF- κ B signaling in response to diabetes or hyperglycemic conditions is an established driver of retinal disease.^{19–23} In addition to enhancing *Nlrp3* mRNA expression, NF- κ B also promotes the transcription of mRNAs that encode an array of cytokines and chemokines, in addition to IL-1 β .²⁴ Canonical NF- κ B signaling is controlled by inhibitor of κ B (I κ B), which sequesters the transcription factor in the cytoplasm.²⁵ I κ B kinase (IKK) phosphorylates I κ B to promote its proteasomal degradation, allowing both IKK-dependent phosphorylation of NF- κ B at S536 and NF- κ B nuclear translocation.^{26,27} We recently demonstrated that, in a preclinical rodent model of diabetes, retinal NF- κ B activity was enhanced in coordination with activation of IKK and decreased I κ B expression.²⁸ Moreover, we discovered that expression of the stress response protein regulated in development and DNA damage response 1 (REDD1, also known as *DDIT4*/*RTP801*) was critical for diabetes-induced NF- κ B signaling and retinal immune cell activation in the retina.²⁸ Specifically, diabetes enhanced REDD1-dependent activation of the kinase GSK3 β to promote canonical activation of NF- κ B.²⁹

Prior studies support that caspase-1 in the retina of mice is localized principally to the inner retinal processes of Müller glia.¹⁶ Müller cells are the most abundant retinal macroglia and provide critical homeostatic, metabolic, and structural support to neurons, photoreceptors, and the vasculature of the retina.³⁰ In response to diabetes, Müller glia become activated and secrete a number of cytokines and growth factors that drive immune cell activation and the development of vascular defects.^{31,32} Notably, REDD1 expression in the retina is also localized to Müller glia.³³ Thus, the studies here were designed to investigate a potential role for REDD1 in retinal NLRP3 inflammasome activation in response to diabetes.

METHODS

Animals

Genetic manipulation of REDD1 was achieved by whole-body knockout (KO) (REDD1^{+/+} vs. REDD1^{-/-}) in B6;129 mice.³⁴ Müller glia-specific ablation was achieved by crossing C57BL/6J hemizygous *Pdgfra-cre* mice obtained from The Jackson Laboratory (Bar Harbor, ME, USA; stock #013148) with floxed REDD1 (REDD1^{fl/fl}) mice to obtain REDD1-mgKO (*Pdgfra-cre*; REDD1^{fl/fl}) C57BL/6J mice, as previously described.³³ Diabetes was induced in mice at 6 weeks of age by administering intraperitoneal injections of STZ for 5 consecutive days. Male and female mice received 50 or 75 mg/kg STZ, respectively, as previously described.³⁵ No sex differences were observed. Equivalent volumes of sodium citrate buffer were administered as a vehicle control. Diabetic phenotype was confirmed 2 weeks after injection and mice were considered diabetic with a fasting blood glucose concentration of >250 mg/dL. Based on our prior work,²⁸ mice were euthanized, and whole eyes or retina were extracted after 16 weeks of diabetes. In some stud-

ies, C57BL/6J mice (Jackson Laboratory) were administered either dapagliflozin (1 mg/kg, Apex Bio, Houston, TX, USA) or vehicle (0.1% DMSO, 0.9% NaCl) for 2 weeks, beginning 14 weeks after STZ administration. Additionally, the GSK3 β inhibitor VP3.15 (10 mg/kg, MedChemExpress, Monmouth Junction NJ, USA) or vehicle (10% DMSO, 0.9% NaCl) was administered to some mice by daily intraperitoneal injections for 3 weeks, beginning 13 weeks after STZ administration. All mice were housed in a 12:12-h reverse light-dark cycle. All animal studies were performed in accordance with the ARVO statement on the ethical use of animals in ophthalmological research and were approved by the Penn State College of Medicine Institutional Animal Care and Use Committee.

Cell Culture

Human MIO-M1 Müller cells were acquired from the UCL Institute of Ophthalmology (London, UK). REDD1 KO MIO-M1 cells were generated by CRISPR-Cas9 genome editing as previously described.³⁶ MIO-M1 cultures were maintained in DMEM (Thermo Fisher Scientific, Waltham, MA, USA) containing 5.6 mM glucose and supplemented with 10% heat-inactivated fetal bovine serum and 1% penicillin-streptomycin. MIO-M1 cells stably expressing an shRNA targeting GSK3 β were generated as previously described.^{29,37} Cells expressing pLKO.1-TRC were used as an shRNA control (Addgene Plasmid #10879). To model hyperglycemic conditions, culture medium was supplemented with D-glucose to achieve a final concentration of 30 mmol/L glucose for up to 24 h. Medium containing 5.6 mM glucose plus 24.4 mM mannitol was used as an osmotic control. Lipofectamine 2000 (Life Technologies, Carlsbad, CA, USA) was used for cell transfection. Plasmids included pCMV5 vector, pCMV-HA-caGSK3 β , and pCMV-HA-REDD1.²⁹ In some studies, cell culture medium was supplemented with 1 μ M IMD0354 (Tocris Biosciences, Bristol, UK) or 1 μ M VP3.15 (MedKoo Biosciences, Durham, NC, USA).

Immunofluorescent Microscopy

Whole eyes were excised and fixed in 4% paraformaldehyde (PFA, pH 7.5) for 30 min. Eyes were washed with 1xPBS and embedded in optimal cutting temperature compound, flash frozen, and sectioned. Cryosections (10 μ m) were fixed in 2% PFA and permeabilized in PBS + 0.1% Triton-X-100 (PBS-T). MIO-M1 cells were cultured on chamber slides (CELLTREAT Scientific Products, Pepperell, MA, USA) for 24 h before exposure to hyperglycemic conditions. Cells were then fixed in 4% PFA and permeabilized with PBS-T. Sections or cell monolayers were then blocked with 10% horse serum and labeled with the appropriate antibodies (Supplementary Table S1). Staining with secondary antibody alone was performed as a negative control (Supplementary Fig. S1). Active caspase-1 was detected using a FAM-FLICA Caspase-1 Kit (Bio-Rad Laboratories, Hercules, CA, USA). Slides were counter stained with either DAPI or Hoeschst33342 and mounted with Fluoromount aqueous mounting media (Sigma-Aldrich, St. Louis, MO, USA). Images were captured by confocal laser microscope (Leica SP8; Leica Biosystems, Wetzlar, Germany) with frame-stack sequential scanning.

Protein Analysis

Retinas were collected as described previously.³⁸ Equal amounts of protein from cell lysates or retinal homogenates were combined with Laemmli buffer, boiled for 5 min, and fractionated using a 4–20% Criterion TGX Precast gel (Bio-Rad Laboratories). Proteins were transferred to a polyvinylidene fluorine membrane, blocked using 5% milk in Tris-buffered saline Tween 20, and incubated with antibodies (Supplementary Table S1). The concentration of IL-1 β was determined in the retina whole cell lysates or in culture medium using the DuoSet mouse (DY401-05) and human (DY201-05) IL-1 β /IL-1F2 ELISA kits (R&D Systems, Minneapolis, MN, USA), respectively.

PCR Analysis

Total RNA was extracted with TRIzol (Invitrogen, Waltham, MA, USA), and 1 μ g of RNA was reverse-transcribed using the High-Capacity cDNA Reverse Transcription Kit (Applied Biosystems, Waltham, MA, USA) and subjected to quantitative real-time PCR (QuantStudio 12K Flex Real-Time PCR System, Thermo Fisher Scientific; RRID:SCR_021098) using Quantitect SYBR Green Master Mix (Qiagen, Hilden, Germany). PCR primer sequences are listed in Table S2. Expression of target mRNAs was normalized to glyceraldehyde 3-phosphate dehydrogenase or actin mRNA using the $2^{-\Delta\Delta CT}$ method.

Visual Function Assessment

Visual function was evaluated using an OptoMotry virtual optomotor system (CerebralMechanics, White Plains, NY,

USA) as previously described.³⁸ Spatial frequency and contrast sensitivity were assessed by elicitation of the optomotor reflex in response to a vertical grating pattern rotating around the mouse on four inward-facing computer monitors. Spatial frequency and contrast sensitivity were evaluated at different parameters using a random step-wise protocol.³⁹ Contrast sensitivity was assessed at a spatial frequency of 0.092 cycles/degree. Spatial frequency was assessed at 100% contrast. Spatial frequency threshold and contrast sensitivity were defined as the highest values to elicit the optomotor reflex. Values were averaged for each mouse over three trials on consecutive days.

Statistical Analyses

Data are expressed as mean \pm SD. One-way ANOVA was used to analyze data from experiments with more than two groups, and pairwise comparisons were made using the Tukey's test for multiple comparisons. Significance between two groups was determined by the Student *t* test. Significance is indicated at a *P* value of <0.05 for all analyses. All *p* values for differences between groups are included in Supplementary Table S3.

RESULTS

Diabetes-Induced Hyperglycemia Increased NLRP3 in the Retina of Diabetic Mice

NLRP3 protein was localized in murine retina by immunofluorescent microscopy (Fig. 1A). STZ-induced diabetes promoted NLRP3 protein content throughout the retinal

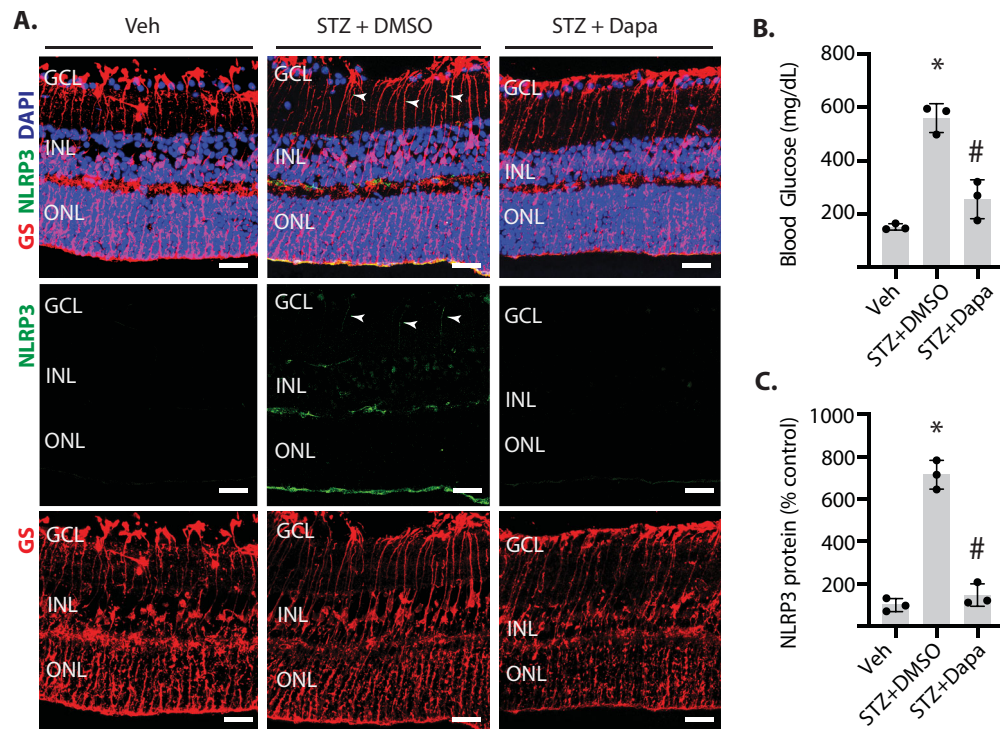


FIGURE 1. Diabetes-induced hyperglycemia promoted NLRP3 expression in the retina. Diabetes was induced in mice by administration of STZ. Control nondiabetic mice received vehicle (Veh). After 14 weeks of diabetes, mice were treated with the SGLT2 inhibitor dapagliflozin or a 0.1% DMSO vehicle daily for 2 additional weeks. (A) NLRP3 (green) and glutamine synthetase (GS, red) was visualized in retinal sections by immunofluorescence. Nuclei were visualized with DAPI (blue). Representative images are shown (scale bar, 25 μ m). Arrowhead indicates

NLRP3 localization to radially oriented cell processes. (B) Fasting blood glucose concentrations were determined. (C) NLRP3 protein in A was quantified. Values are means \pm SD ($n = 3$). * $P < 0.05$ vs. Veh; # $P < 0.05$ vs. STZ + DMSO. GCL, ganglion cell layer; INL, inner nuclear layer; ONL, outer nuclear layer.

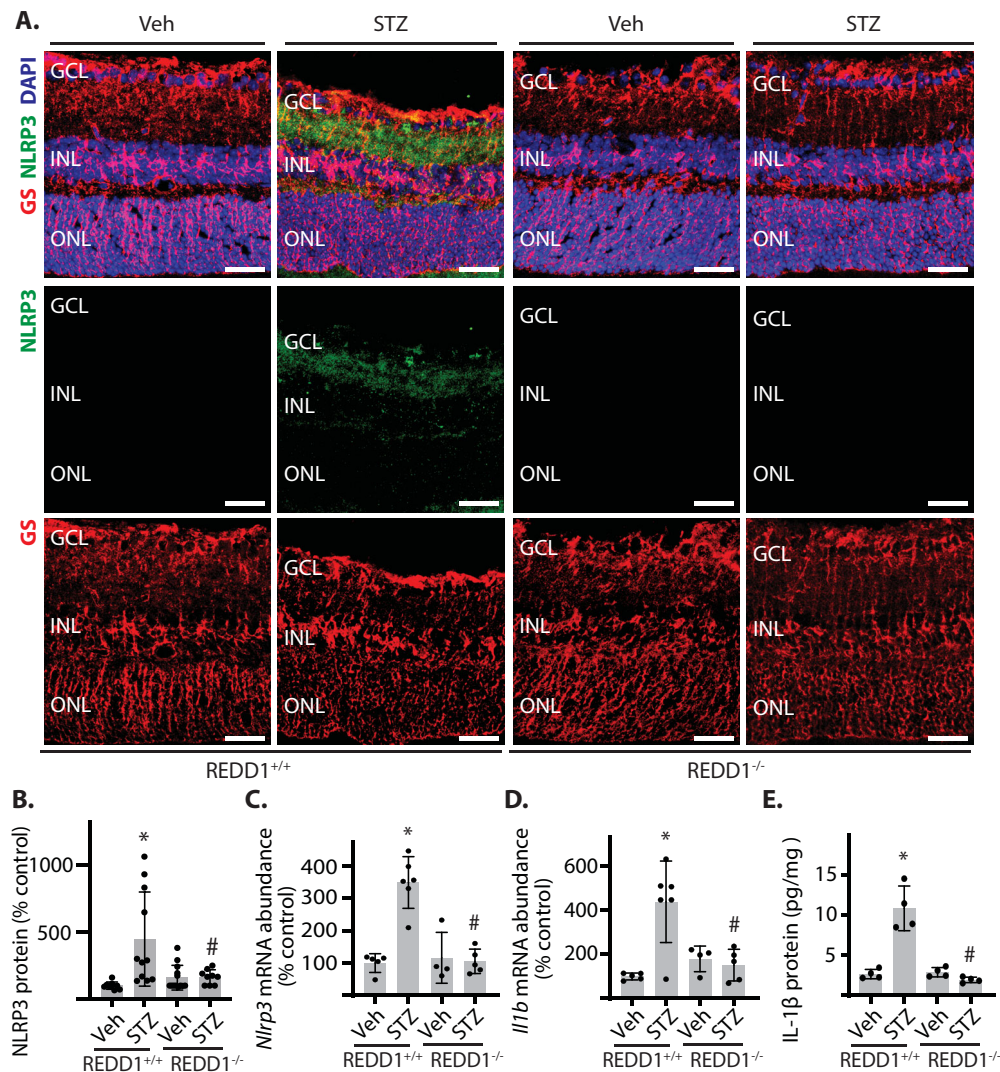


FIGURE 2. REDD1 was required for increased NLRP3 expression in the retina of diabetic mice. Diabetes was induced in REDD1^{+/+} and REDD1^{-/-} mice by administration of STZ. All analyses were performed 16 weeks after administration of STZ or vehicle (Veh). (A) NLRP3 (green) and glutamine synthetase (GS, red) was visualized in retinal sections by immunofluorescence. Nuclei were visualized with DAPI (blue). Representative images are shown (scale bar, 50 μ m). (B) NLRP3 protein in (A) was quantified. (C–D) *Nlrp3* and *Il1b* mRNA expression were determined in retina tissue homogenate by RT-PCR. (E) IL-1 β protein content in retinal lysates was quantified by ELISA. Values are means \pm SD ($n = 4$ –11). * $P < 0.05$ vs. Veh; # $P < 0.05$ vs. REDD1^{+/+}. GCL, ganglion cell layer; INL, inner nuclear layer; ONL, outer nuclear layer.

layers. NLRP3 was partially localized to radially oriented cell processes within the inner retina. Significant co-localization of NLRP3 with the Müller cell marker glutamine synthetase supported diabetes-induced upregulation of NLRP3 specifically in Müller glia. Retinal NLRP3 expression was also evaluated in retina by analysis of single-cell RNA sequencing data. NLRP3 expression in retinal cell clusters was greatest in Müller glia (Supplementary Fig. S2). To specifically evaluate the impact of hyperglycemia on diabetes-induced NLRP3, blood glucose concentrations were normalized in diabetic mice by the induction of glucosuria with dapagliflozin. Daily dapagliflozin treatment normalized blood glucose levels in diabetic mice independently of insulin (Fig. 1B). Normaliza-

tion of blood glucose concentrations reduced retinal NLRP3 protein content in the retina of diabetic mice, such that it was no longer elevated as compared with nondiabetic mice (Fig. 1C).

REDD1 Deletion Prevented an Increase in NLRP3 in the Retina of Diabetic Mice

We previously demonstrated that STZ-induced diabetes enhanced retinal inflammation in a REDD1-dependent manner.²⁸ To evaluate the impact of REDD1 on diabetes-induced NLRP3 upregulation, retinas from REDD1^{+/+} and REDD1^{-/-} mice were analyzed. Fasting blood glucose

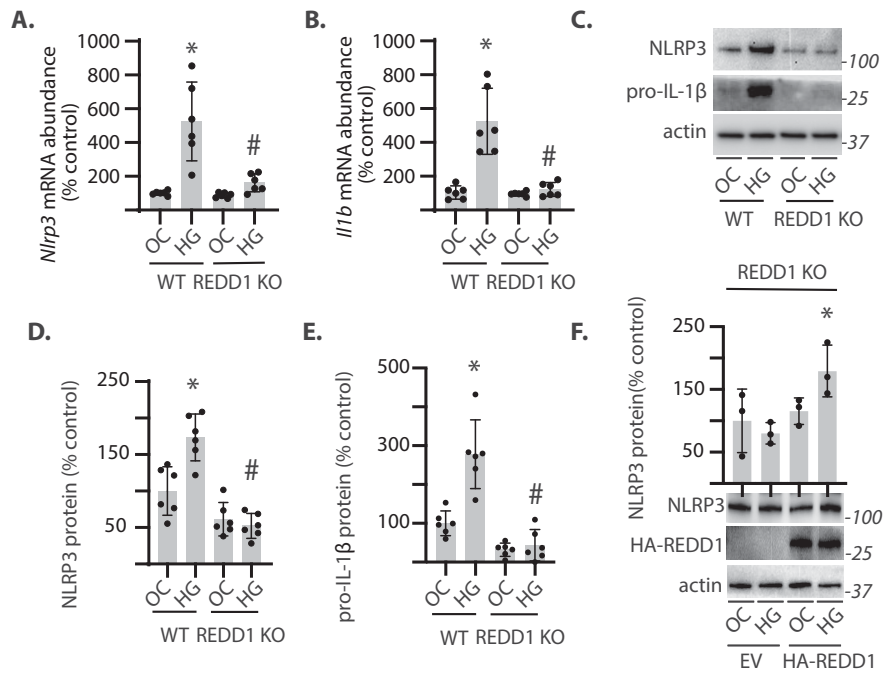


FIGURE 3. REDD1 deletion reduced NLRP3 expression in Müller cell cultures exposed to hyperglycemic conditions. Wild-type (WT) and REDD1 KO human MIO-M1 cells were cultured in medium containing 5.6 mM glucose and exposed to medium containing either 30 mM glucose (HG) or an osmotic control (OC) containing 5.6 mM glucose plus 24.4 mM mannitol for 24 h. (A and B) *Nlrp3* and *Il1b* mRNA expression were determined in cell lysates by RT-PCR. (C–E) NLRP3 and pro-IL-1 β protein abundance was determined in cell lysates by western blotting. Representative blots are shown. Molecular mass in kDa is indicated at right of each blot. Quantification of blots in (C) are shown in (D) and (E). (F) NLRP3 protein abundance was evaluated in REDD1 KO cells expressing either an empty vector control (EV) or hemagglutinin (HA)-tagged REDD1. Values are means \pm SD ($n = 3-6$). * $P < 0.05$ vs. OC; # $P < 0.05$ vs. WT or EV.

concentrations were similar in diabetic REDD1^{+/+} and REDD1^{-/-} mice (Supplementary Table S4). In response to diabetes, NLRP3 protein was increased in the retina of REDD1^{+/+} mice, with staining most concentrated in the inner retinal layers (Figs. 2A, B). In contrast with diabetic REDD1^{+/+} mice, NLRP3 protein was not increased in the retina of diabetic REDD1^{-/-} mice. Diabetic REDD1^{+/+} mice also exhibited an increase in *Nlrp3* mRNA expression in retinal tissue homogenates, which was prevented by REDD1 deletion (Fig. 2C). Consistent with the change in NLRP3, *Il1b* mRNA expression was also increased in the retina of diabetic mice in a REDD1-dependent manner (Fig. 2D). Diabetes also promoted IL-1 β protein content in retina of REDD1^{+/+} mice, but a similar increase was not detected in diabetic REDD1^{-/-} mice (Fig. 2E).

REDD1 Was Required for Increased NLRP3 Expression in Müller Cells Exposed to Hyperglycemic Conditions

To explore a role for REDD1 in NLRP3 inflammasome priming in human Müller glia, wild-type and REDD1 KO MIO-M1 cells were exposed to culture medium supplemented with elevated glucose concentrations as a model for the hyperglycemic conditions seen in the context of diabetes. In wild-type cells, hyperglycemic conditions promoted *Nlrp3* and *Il1b* mRNA expression (Figs. 3A, B). In the absence of hyperglycemic conditions, *Nlrp3* and *Il1b* mRNA expression was similar in wild-type and REDD1 KO cells. In contrast with wild-type cells, REDD1-deficient Müller cells did not exhibit a change in *Nlrp3* and *Il1b* mRNA expression in

response to hyperglycemic conditions. Consistent with the increase in mRNA expression, NLRP3 and pro-IL-1 β protein were enhanced in cells exposed to hyperglycemic conditions and REDD1 was necessary for the effect (Figs. 3C–E). To confirm the role of REDD1 in NLRP3 upregulation, REDD1 expression was rescued in REDD1-deficient cells by ectopic expression of an HA-tagged REDD1 protein. HA-REDD1 was sufficient to restore the increase in NLRP3 protein levels in REDD1 KO cells exposed to hyperglycemic conditions (Fig. 3F).

REDD1 Deletion Reduced Caspase-1 Activation in Müller Cells Exposed to Hyperglycemic Conditions

IL-1 β is released from cells as part a proinflammatory form of cell death known as pyroptosis.⁴⁰ Markers of pyroptosis include pro-caspase-1 cleavage, IL-1 β processing, and Gasdermin D cleavage. In wild-type Müller cells, cleaved caspase-1, IL-1 β processing, and Gasdermin D cleavage were all elevated upon exposure to hyperglycemic conditions in coordination with an increase in REDD1 (Fig. 4A). By contrast, REDD1-deficient cells did not exhibit a change in cleaved caspase-1, mature IL-1 β , or the Gasdermin D N-terminal cleavage product. In wild-type cells exposed to hyperglycemic conditions, an increase in active caspase-1 was also demonstrated by enhanced labeling of cells with a fluorescent peptide inhibitor that irreversibly binds the active enzyme (Figs. 4B, C). Unlike wild-type cells, increased caspase-1 activity was not observed in REDD1-deficient cells exposed to hyperglycemic conditions. In wild-

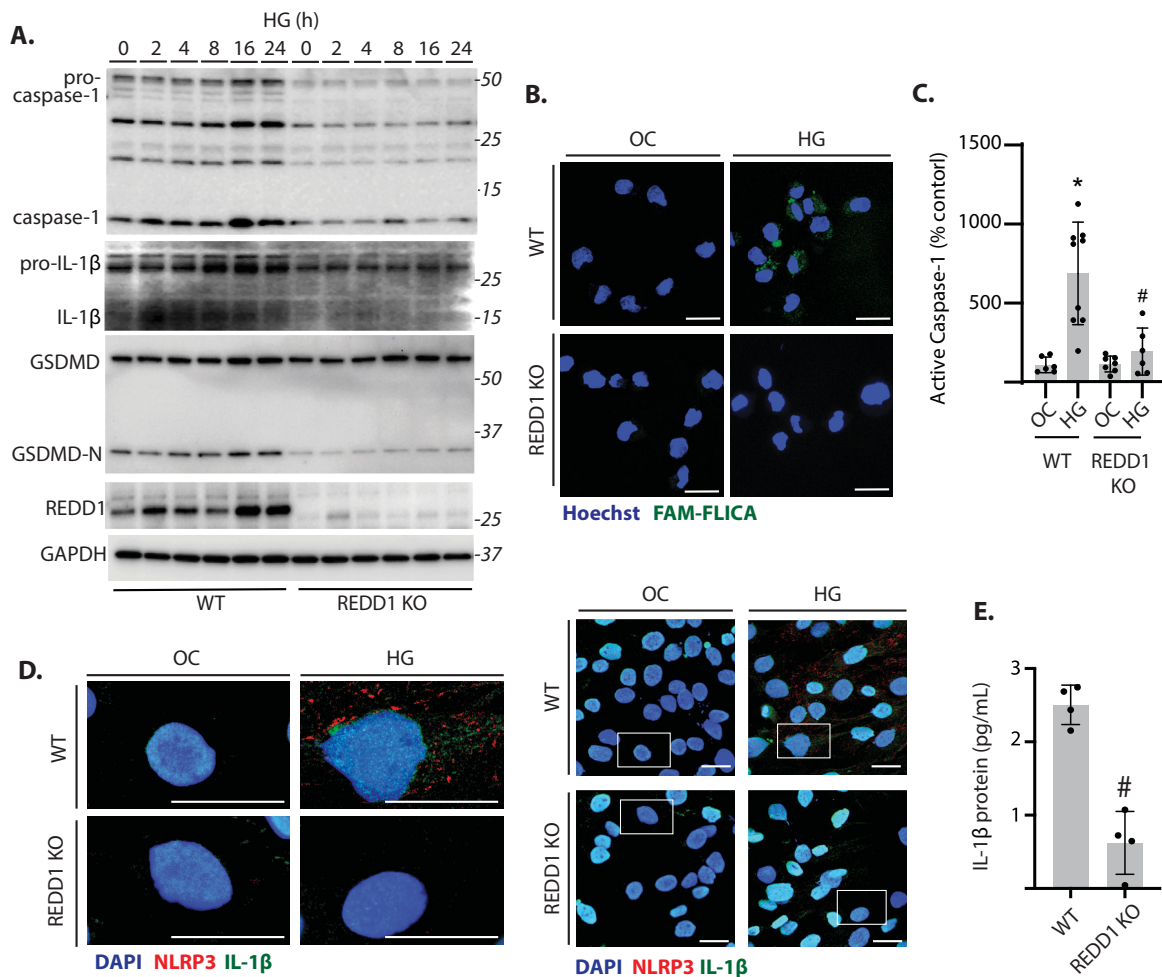


FIGURE 4. REDD1 deletion reduced caspase-1 activation in Müller cells exposed to hyperglycemic conditions. Wild-type (WT) and REDD1 KO human MIO-M1 cells were cultured in medium containing 5.6 mM glucose and exposed to medium containing either 30 mM glucose (HG) or an osmotic control (OC) containing 5.6 mM glucose plus 24.4 mM mannitol for 24 h. (A) Caspase-1, IL-1 β , Gasdermin D (GSDMD), and REDD1 were evaluated in cell lysates by western blotting after up to 24 h exposure to HG. (B and C) Active caspase-1 was visualized by immunofluorescence via labeling with the inhibitor probe FAM-YVAD-FMK (green) after 24 h exposure to OC or HG (scale bar, 25 μ m). Nuclei were counterstained with Hoechst 33342. Representative images are shown in (B). (D) NLRP3 (red) and IL-1 β (green) protein was visualized in cells by immunofluorescence after 24 h exposure to LG or HG (scale bar, 25 μ m). Nuclei were visualized with DAPI. White box indicates area shown at increased magnification at left. (E) IL-1 β secretion was evaluated by quantifying IL-1 β levels present in cell culture medium after 24 h of exposure to HG by ELISA. Values are means \pm SD ($n = 4-9$). * $P < 0.05$ vs. OC; # $P < 0.05$ vs. WT; GSDMD-N, N-terminal GSDMD cleavage product.

type cells exposed to hyperglycemic conditions, increased NLRP3 protein was localized to distinct puncta throughout the cytosol, which were absent in REDD1 KO cells (Fig. 4D). An increase in IL-1 β upon exposure to hyperglycemic conditions was also observed by immunofluorescence in wild-type, and not REDD1 KO, cells. To evaluate IL-1 β release, the cytokine was measured in cell culture medium by ELISA. IL-1 β in medium from cells exposed to hyperglycemic conditions was reduced by REDD1 deletion (Fig. 4E).

NF- κ B Signaling Was Required for Increased NLRP3 Expression in Response to Hyperglycemic Conditions

We then investigated a role for REDD1-dependent NF- κ B signaling as a driver of NLRP3. I κ B protein was reduced in cells exposed to hyperglycemic conditions, and REDD1 was required for the decrease (Fig. 5A). Consistent

with the reduction in I κ B, IKK α/β autophosphorylation at S176/S180 was also enhanced in wild-type cells exposed to hyperglycemic conditions (Fig. 5B). Unlike wild-type cells, REDD1-deficient cells did not exhibit enhanced IKK autophosphorylation in response to hyperglycemic conditions (Fig. 5B). To evaluate a role for REDD1-dependent IKK activation in NLRP3 expression, IKK kinase activity was inhibited by exposure to IMD0534. Although *Nlrp3* and *Il1b* mRNA expression was increased upon exposure to hyperglycemic conditions, IKK β inhibition prevented the effect (Figs. 5C, D). The data demonstrate a role for REDD1-dependent IKK activation in promoting NLRP3 expression.

REDD1-Dependent GSK3 β Signaling Promoted NLRP3 Inflammasome Priming

In support of the prior report,²⁹ NF- κ B phosphorylation at S536 was enhanced in response to hyperglycemic condi-

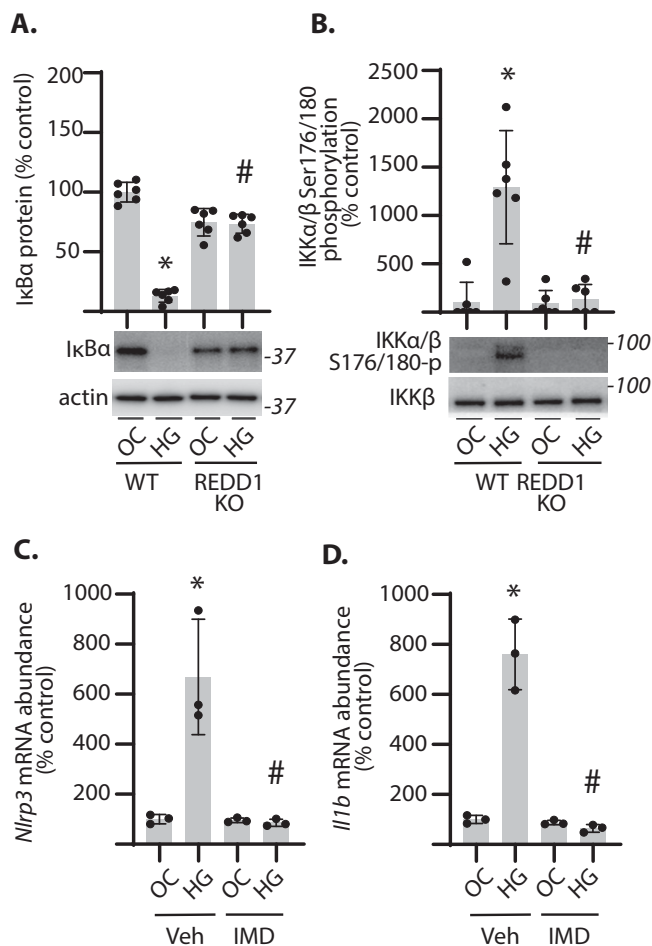


FIGURE 5. IKK activity was required for REDD1-dependent NLRP3 upregulation in Müller cells exposed to hyperglycemic conditions. Wild-type (WT) and REDD1 KO human MIO-M1 cells were cultured in medium containing 5.6 mM glucose and exposed to medium containing either 30 mM glucose (HG) or an osmotic control (OC) containing 5.6 mM glucose plus 24.4 mM mannitol for 24 h. (A and B) *IκBα* protein abundance and phosphorylation of *IKKα/β* at S176/180 were determined in cell lysates by western blotting. Representative blots are shown. Molecular mass in kDa is indicated at *right* of each blot. (C and D) Cells were exposed to culture medium supplemented with either the IKK inhibitor IMD0534 (IMD) or a vehicle control (Veh). Abundance of mRNAs encoding *Nlrp3* (C) and *Il1b* (D) was determined in cell lysates by RT-PCR. Values are means \pm SD ($n = 3-6$). * $P < 0.05$ vs. OC; # $P < 0.05$ vs. WT or Veh.

tions coincident with increased glycogen synthetase phosphorylation at S641 and reduced inhibitory phosphorylation of GSK3 β at S9 (Fig. 6A). Importantly, REDD1 was required for these changes in phosphorylation in response to hyperglycemic conditions. To evaluate a role for GSK3 β in regulation of NLRP3, an shRNA was used to knockdown GSK3 β expression (Fig. 6B). GSK3 β knockdown attenuated NLRP3 protein abundance and NF- κ B phosphorylation at S536 in cells exposed to hyperglycemic conditions (Fig. 6C). GSK3 β knockdown also prevented an increase in *Nlrp3* and *Il1b* mRNA expression upon exposure to hyperglycemic conditions (Figs. 6D, E). Consistent with the suppressive effect of genetic GSK3 β suppression, GSK3 inhibition with VP3.15 also prevented an increase in *Nlrp3* and *Il1b* mRNA expression in cells exposed to hyperglycemic conditions (Figs. 6F, G). GSK3 β activity was then rescued in REDD1-

deficient Müller cells by expression of a constitutively active GSK3 β^{S9A} variant protein. GSK3 β^{S9A} expression was sufficient to enhance both *Nlrp3* and *Il1b* mRNA expression in REDD1-cells (Figs. 6I, J). The data support a role for REDD1-dependent GSK3 β activation in promoting NLRP3 inflammasome priming.

GSK3 Suppression Prevented Increased NLRP3 Expression in the Retina of Diabetic Mice

To investigate a role for GSK3 in diabetes-induced NLRP3 inflammasome priming, 13-weeks after STZ administration, diabetic mice were administered daily intraperitoneal injections of VP3.15 for 3 weeks. Fasted blood glucose concentrations were elevated by diabetes and unaffected by treatment with VP3.15 (Supplementary Table S4). Diabetes promoted retinal *Nlrp3* mRNA expression and VP3.15 prevented the increase (Fig. 7A). NLRP3 protein abundance was also increased throughout the inner and outer retina of diabetic mice, and VP3.15 attenuated diabetes-induced NLRP3 protein abundance (Fig. 7B). Similarly, diabetic mice exhibited increased retinal *Il1b* mRNA expression, and VP3.15 prevented the effect (Fig. 7C). IL-1B protein was elevated in retinal tissue homogenates from diabetic mice, and VP3.15 treatment reduced IL-1B protein abundance (Fig. 7D). Overall, these data support that GSK3 activation is necessary for NLRP3 inflammasome priming in the retina of diabetic mice.

Müller Cell-Specific REDD1 Deletion Prevented Increased Retinal NLRP3 Protein and Contrast Sensitivity Deficits in Diabetic Mice

To investigate a role for REDD1 expression specifically in Müller glia in retinal dysfunction, REDD1^{fl/fl} and REDD1 mgKO mice were evaluated after 16 weeks of STZ-induced diabetes. Diabetes increased fasted blood glucose concentrations in both REDD1^{fl/fl} mice and REDD1 mgKO mice to a similar extent (Supplementary Table S4). Diabetic REDD1^{fl/fl} mice exhibited increased NLRP3 protein abundance throughout the retina, whereas Müller glia-specific deletion of REDD1 prevented retinal NLRP3 accumulation (Fig. 8A, B). Functional vision was assessed by measurement of the optomotor response. Diabetic REDD1^{fl/fl} mice exhibited significant deficits in both spatial frequency threshold (Fig. 8C) and contrast sensitivity (Fig. 8D) as compared with nondiabetic REDD1^{fl/fl} mice. Spatial frequency thresholds were also reduced in diabetic REDD1 mgKO mice as compared with nondiabetic mgKO mice. Contrast sensitivity was not different in diabetic and nondiabetic REDD1 mgKO mice. Together the data support a role for Müller glia-specific REDD1 expression in diabetes-induced NLRP3 upregulation and visual function deficits in contrast sensitivity.

DISCUSSION

Studies here delineate molecular mechanisms that contribute to retinal NLRP3 inflammasome activation in the context of diabetes. Diabetes suppresses the normally rapid degradation of REDD1 protein, leading to increased REDD1 protein abundance in the retina.⁴¹ We recently demonstrated that the increase in REDD1 was required for immune cell activation and proinflammatory cytokine expression in the retina of diabetic mice.^{28,29} Here, REDD1

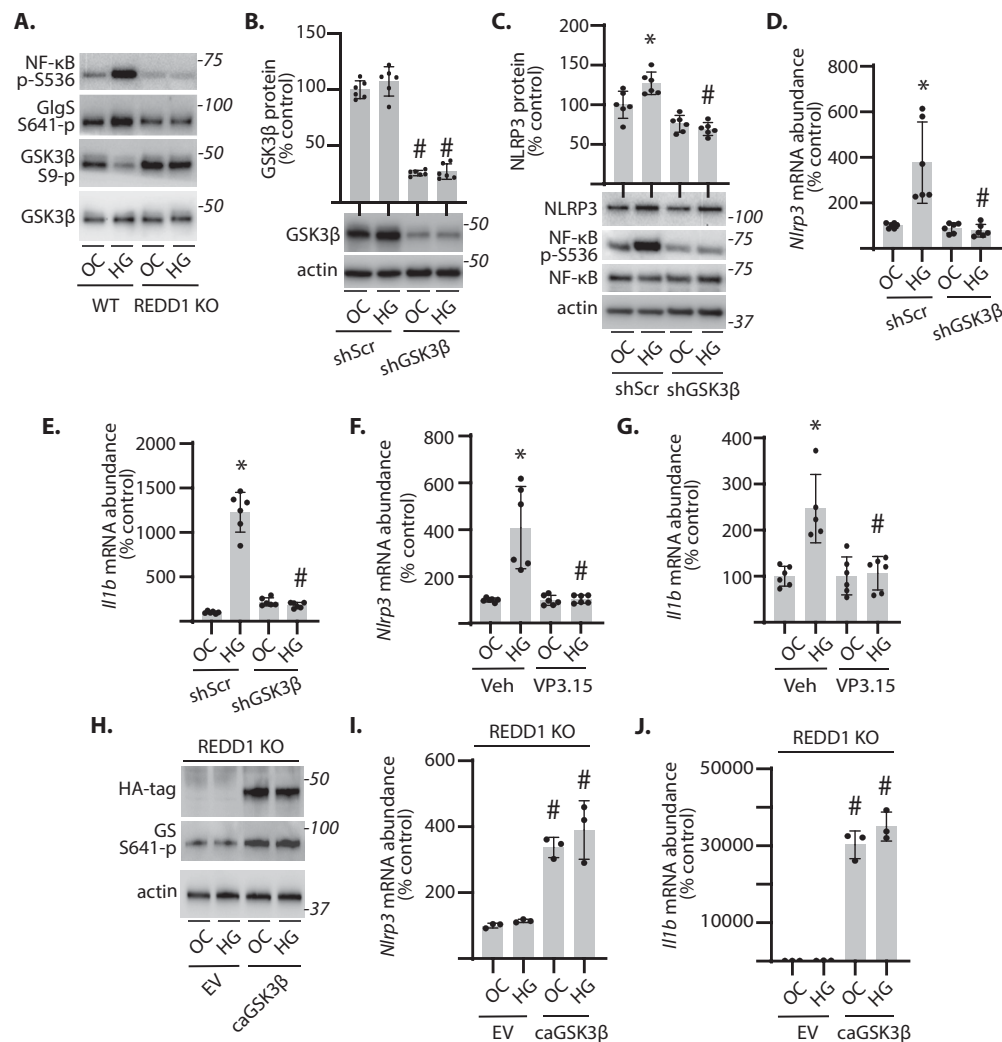


FIGURE 6. GSK3 β was necessary and sufficient for increased NLRP3 expression in Müller cells exposed to hyperglycemic conditions. Wild-type (WT) and REDD1 KO human MIO-M1 cells were cultured in medium containing 5.6 mM glucose and exposed to medium containing either 30 mM glucose (HG) or an osmotic control (OC) containing 5.6 mM glucose plus 24.4 mM mannitol for 24 h. (A) Phosphorylation of NF- κ B at S536, glycogen synthase (GlgS) at S641, and GSK3 β at S9 was determined in cell lysates by western blotting. Representative blots are shown. Molecular mass in kDa is indicated at right of each blot. (B–E) GSK3 β mRNA expression was knocked down in WT cells by stable expression of an shRNA (shGSK3 β). Control cells expressed a scramble shRNA (shScr). Western blotting was used to evaluate GSK3 β (B), NLRP3 (C), and NF- κ B phosphorylation at S536. Abundance of mRNAs encoding *Nlrp3* (D) and *Il1b* (E) was determined in cell lysates by RT-PCR. (F and G) WT cells were exposed to culture medium supplemented with either the GSK3 inhibitor VP3.15 or a vehicle control (Veh). (H–J) REDD1 KO cells were transfected to express either empty vector control (EV) or a hemagglutinin (HA)-tagged constitutively active GSK3 β S9A variant (caGSK3 β). Values are means \pm SD ($n = 3$ –6). * $P < 0.05$ vs. OC; # $P < 0.05$ vs. shScr, Veh, or EV.

was required for the upregulation of NLRP3 in both the retina of diabetic mice and in retinal Müller glia exposed to hyperglycemic conditions. REDD1 was necessary for transcriptional priming of the NLRP3 inflammasome and enhanced IL-1 β in the retina of diabetic mice. Moreover, REDD1 deletion prevented caspase-1 activation and reduced IL-1 β secretion in Müller cells exposed to hyperglycemic conditions. Overall, the data support a working model wherein REDD1 promotes diabetes-induced GSK3 β dephosphorylation, IKK activation, and NF- κ B nuclear localization to enhance NLRP3 inflammasome activity in the retina (Supplementary Fig. S5).

After 16 weeks of STZ-induced diabetes, increased NLRP3 protein abundance was observed throughout the retina. A similar increase in retinal NLRP3 is seen in retinal cross sections from diabetic *Ins2^{Akita}* mice, as well as in

the double transgenic Akimba (*Ins2^{Akita};VEGF^{+/-}*) mice.¹⁷ NLRP3 protein is also upregulated in retinal lysates from STZ-induced diabetic rats.¹³ Colocalization of NLRP3 in the retina of diabetic mice with the Müller cell marker glutamine synthetase supports that the increase in retinal NLRP3 content with diabetes was partially localized to Müller glia. The observation supports prior reports that Müller cells are a source for NLRP3 in the retina.^{42,43} The diabetes-induced increase in retinal NLRP3 was mediated by hyperglycemia, as normalization of blood glucose concentration prevented the effect. The observation is consistent with prior studies demonstrating that normalization of blood glucose levels in diabetic rodents by the induction of glucosuria is sufficient to prevent upregulation of REDD1, Müller cell gliosis, and retinal neurodegeneration.^{44,45} Notably, NLRP3 expression is specifically increased in Müller cells exposed to hyper-

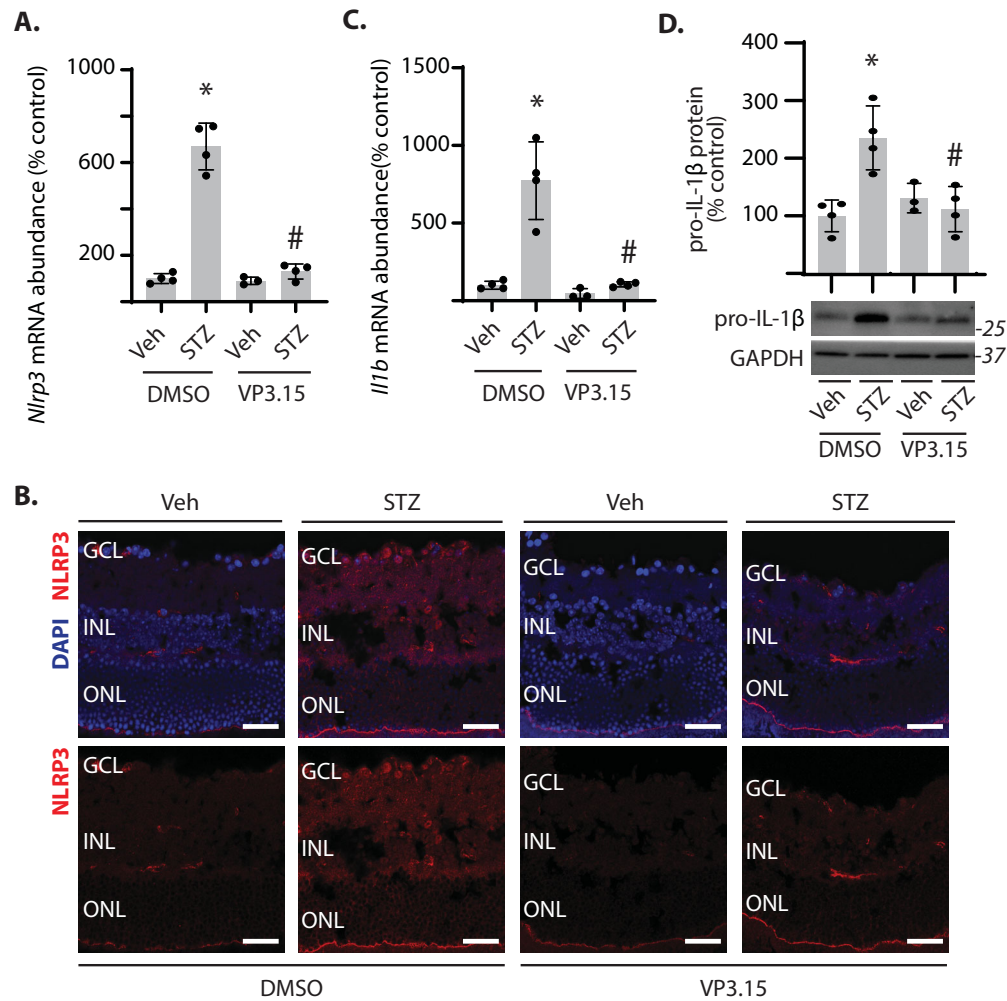


FIGURE 7. GSK3 inhibition prevented diabetes-induced NLRP3 inflammasome priming in the retina. Diabetes was induced in mice by administration of STZ. All analyses were performed 16 weeks after mice were administered STZ or a vehicle (Veh). During the last 3 weeks of diabetes, mice were treated daily by intraperitoneal administration of the GSK3 inhibitor VP3.15 or a vehicle (10% DMSO). **(A)** *Nlrp3* mRNA expression was determined in retinal tissue homogenates by RT-PCR. **(B)** NLRP3 protein (red) was visualized in retinal sections by immunofluorescence. DAPI (blue) was used to visualize nuclei. Representative micrographs are shown (scale bar, 50 μ m). **(C)** *Il1b* mRNA expression was determined in retinal tissue homogenates by RT-PCR. **(D)** Pro-IL-1 β protein abundance was determined in retinal tissue homogenates by western blotting. Representative blots are shown. Molecular mass in kDa is indicated at right of each blot. Values are means \pm SD ($n = 3-4$). * $p < 0.05$ vs. Veh; # $p < 0.05$ vs. DMSO. GCL, ganglion cell layer; INL, inner nuclear layer; ONL, outer nuclear layer.

glycemic conditions, whereas other inflammasome sensors, including NLRP1, NLRC4, and AIM2, are not changed.¹² Importantly, the data here do not support that the increase in retinal NLRP3 content with diabetes is exclusively localized to Müller glia. However, Müller glia-specific REDD1 deletion was sufficient to prevent increased NLRP3 throughout the entire retina of STZ-induced diabetic mice. Because Müller glia-specific REDD1 was required for NLRP3 upregulation throughout the entire retina, the data support that diabetes-induced signaling events specifically in Müller cells are necessary for NLRP3 upregulation in other cells of the retina.

Caspase-1 activation and increased IL-1 β production have long been known to contribute to diabetes-induced retinal pathology.⁴ In the retina of diabetic mice, caspase-1 is principally localized to Müller glia.¹⁶ Similarly, REDD1 expression in both human and rodent retina is dominant in Müller glia.³³ Müller glia play a central role in the development of retinal inflammation, as they become gliotic in response to

diabetes and secrete a range of extracellular modulators that activate the immune response.^{31,32} It is well established that caspase-1 activity and IL-1 β processing are upregulated in Müller cells exposed to hyperglycemic conditions.^{4,12} The studies here extend on the prior reports by demonstrating a role for REDD1 in promoting caspase-1 activation and IL-1 β secretion. Notably, other important signaling pathways are also known to contribute to caspase-1 activation.⁴⁶ For example, caspase-4 and caspase-5 (and caspase-11 in mice) are activated by cytosolic lipopolysaccharide from bacteria⁴⁷ as well as in models of diabetic nephropathy⁴⁸ and could also play a role in the pathogenesis of diabetic retinopathy by promoting the activation of caspase-1.

Increased NLRP3 expression in Müller cells exposed to hyperglycemic culture conditions is mediated by activation of NF- κ B, which binds the NLRP3 promoter to enhance transcriptional priming.⁴² In both Müller cells exposed to hyperglycemic conditions and in the retina of diabetic mice, NF- κ B activity is enhanced in a REDD1-dependent manner.^{28,29} We

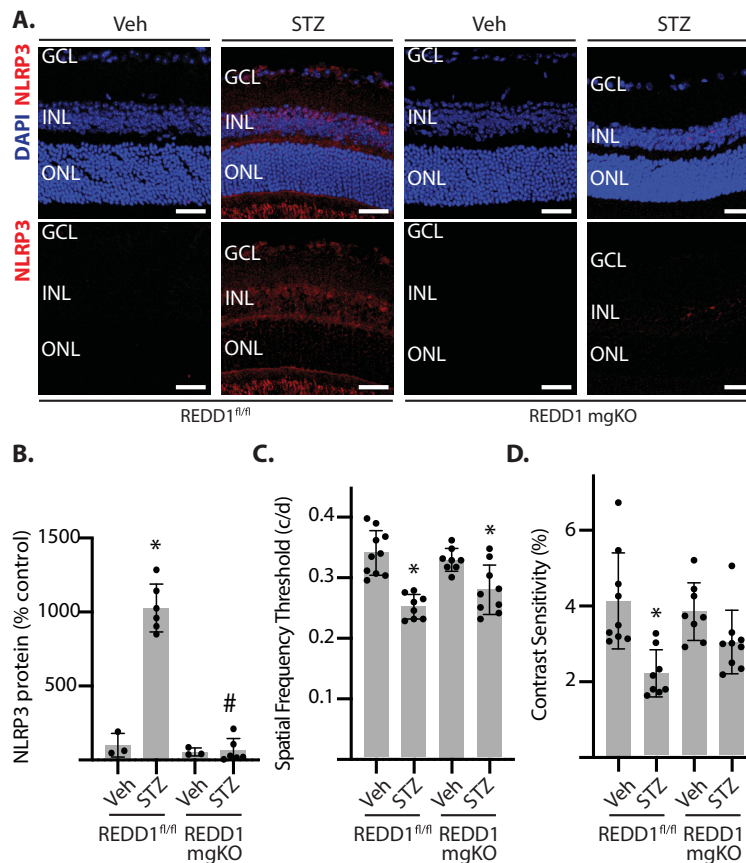


FIGURE 8. Diabetes-induced retinal NLRP3 expression and contrast sensitivity deficits were absent in mice with Müller glia-specific REDD1 deletion. Diabetes was induced in REDD1^{fl/fl} and REDD1 mgKO mice by administration of STZ. Control mice received a vehicle (Veh). All analyses were performed after 16 weeks of diabetes. (A) NLRP3 protein (red) was visualized in retinal sections by immunofluorescence. DAPI (blue) was used to visualize nuclei. Representative micrographs are shown (scale bar, 50 μ m). (B) NLRP3 protein in (A) was quantified. (C and D) Behavioral optometry was performed by displaying rotating bars on a monitor to elicit an optomotor reflex. Thresholds were averaged over three trials on consecutive days. Spatial frequency threshold was assessed at 100% contrast. Contrast sensitivity was assessed at a spatial frequency of 0.092 cycles/degree. Contrast sensitivity is expressed as an inverse percentage to make data interpretation more intuitive. Values are means \pm SD ($n = 3-9$). * $P \leq 0.05$ vs Veh. # $P \leq 0.05$ vs REDD1^{fl/fl}. GCL, ganglion cell layer; INL, inner nuclear layer; ONL, outer nuclear layer.

recently demonstrated that REDD1 promoted canonical NF- κ B signaling in Müller cells exposed to TNF α by enhancing IKK activation and consequently sustaining the reduction in I κ B.²⁸ Extending on the prior report, we found that REDD1 was also necessary for enhanced IKK autophosphorylation and reduced I κ B levels in Müller cells exposed to hyperglycemic conditions. REDD1 deletion prevented increased NLRP3 expression in Müller cells exposed to hyperglycemic conditions, and IKK inhibition produced a similar suppressive effect.

In addition to IKK activity, the increase in NLRP3 in Müller cells exposed to hyperglycemic conditions was also dependent on GSK3 β . Prior studies support a key role for GSK3 β in immune signaling, as the kinase has been implicated in both development and resolution of inflammation.⁴⁹ REDD1 promotes GSK3 β activity by indirectly preventing the inhibitory phosphorylation of GSK3 β at S9. In both the retina of diabetic mice and in Müller cells exposed to hyperglycemic conditions, REDD1 is necessary for GSK3 β dephosphorylation at S9.²⁹ REDD1 recruits protein phosphatase 2A to Akt to facilitate site-specific dephosphorylation at T308 and reduced Akt kinase activity.⁵⁰ In turn, Akt-dependent phosphorylation of GSK3 β at S9 inactivates the kinase.⁵¹

Thus, REDD1 enhances NLRP3 inflammasome activation via an Akt/GSK3 β /NF- κ B signaling axis.

In the retina of diabetic mice treated with the GSK3 inhibitor VP3.15, NLRP3 expression was not increased as compared with nondiabetic control mice. We recently provided evidence that treatment with VP3.15 is sufficient to prevent an increase in glycogen synthase phosphorylation in the retina of diabetic mice.²⁹ Importantly, VP3.15 also prevents an increase in proinflammatory cytokine expression and immune cell activation in the retina of diabetic mice.²⁹ A suppressive effect of GSK3 β inhibition on NLRP3 inflammasome activation was previously demonstrated in a mouse models of lupus nephritis,⁵² ischemia-reperfusion injury,⁵³ and myocardial infarct.⁵⁴ The specific mechanism(s) responsible for GSK3 β -dependent NLRP3 inflammasome activation has not been thoroughly defined; however, a prior study suggested a permissive role for downregulation of autophagy in the effect.⁵³ More recently, GSK3 β was also implicated in sustaining NLRP3 oligomerization.⁵⁵ The studies here support a role for REDD1-dependent activation of GSK3 β as a key driver of increased *Nlrp3* and *Il1b* mRNA expression in both the retina of diabetic mice and in Müller cells exposed to hyperglycemic conditions. Thus,

GSK3 β may contribute to NLRP3 inflammasome activation by impacting both priming and complex assembly.

Studies here provide additional support that diabetes-induced REDD1 contributes to the development of functional deficits in vision. Specifically, a protective effect on contrast sensitivity was observed in the retina of diabetic mice with Müller glia-specific REDD1 deletion, coincident with the absence of an increase in retinal NLRP3 expression. Notably, neither spatial frequency nor contrast sensitivity are impaired in the retina of diabetic REDD1^{-/-} mice as compared with nondiabetic REDD1^{-/-} mice.⁵⁶ However, older nondiabetic REDD1^{-/-} mice develop modest deficits in spatial frequency threshold as compared with nondiabetic REDD1^{+/+} mice, which likely results from reduced glucose and insulin tolerance.^{56,57} Thus, the prior observation did not indicate a protective effect of whole body REDD1 deletion on spatial frequency, but rather the absence of an additive diabetes-induced deficit in older REDD1^{-/-} mice.⁵⁶ We previously demonstrated that deficits in both visual acuity and spatial frequency threshold are not observed in mice with Müller glia-specific REDD1 deletion after 6 weeks of STZ-induced diabetes.³³ After 6 weeks of STZ-induced diabetes, REDD1^{fl/fl} mice exhibit retinal gliosis, neurodegeneration, and deficits in both visual acuity and contrast sensitivity. By contrast, REDD1 mgKO mice were protected from these diabetes-induced retinal defects. To determine if the protective effects of Müller glia-specific REDD1 deletion on visual acuity were maintained in older REDD1 mgKO mice, the studies here extended the duration of STZ-induced diabetes to 16 weeks. Visual acuity and contrast sensitivity were maintained in nondiabetic REDD1 mgKO mice as compared with nondiabetic REDD1^{fl/fl}. Whereas we previously observed a protective effect of REDD1 mgKO on visual acuity after 6 weeks of STZ-induced diabetes,³³ visual acuity was attenuated in REDD1 mgKO mice after 16 weeks of STZ-induced diabetes as compared with nondiabetic mgKO mice. In a post hoc analysis, a trend toward improvement in spatial frequency threshold was observed in diabetic REDD1 mgKO mice as compared with diabetic REDD1^{fl/fl} mice (Supplementary Fig. S3). As in our prior studies, the protective effect of REDD1 deletion was principally observed in contrast sensitivity, which is associated with inner retinal information processing.

There is presently an unmet clinical need for therapeutics that target the initiating molecular events that cause retinal complications. Diabetic retinopathy is clinically defined by vascular changes in the retina; however, NLRP3 inflammasome activation precedes the visible signs of microvascular disease in diabetic patients.⁵⁸ NLRP3 protein is upregulated in the inner retina of diabetic patients without retinopathy, and further increases throughout the entire retina in diabetic patients with diabetic retinopathy.⁵⁸ A similar increase in NLRP3 and IL-1 β protein was previously reported in both vitreous samples and fibrovascular membranes from patients with diabetic retinopathy.^{14,59} Notably, cleaved caspase-1 levels are not elevated in donor retina from diabetic patients without retinopathy as compared with nondiabetic patients.⁵⁸ By contrast, an increase in caspase-1 cleavage in donor retina coincides with the onset of retinal disease, demonstrating that early NLRP3 priming precedes retinal NLRP3 inflammasome activation.⁵⁸ Indeed, in the healthy retina, NLRP3 and IL-1 β expression is minimal, and priming likely represents a key early event in NLRP3 inflammasome activation with disease progression. The proof-of-concept studies here specifically demonstrate that a REDD1-GSK3 β -

NF- κ B signaling axis contributes to diabetes-induced NLRP3 priming and upregulation of IL-1 β in the retina. Overall, the findings support interventions targeting REDD1 as a therapeutic strategy to address the development of retinal complications caused by diabetes.

Acknowledgments

The authors thank Elena Feinstein (Quark Pharmaceuticals) for permission to use the REDD1^{-/-} mice. Parts of this study were presented previously in abstract form at the Association for Research in Vision and Ophthalmology (ARVO) 2023 Annual Meeting, New Orleans, Louisiana, April 22–27, 2023.

Supported by National Institutes of Health grants R01 EY029702, R01 EY032879, and R21 EY035844 (to MDD).

Disclosure: **C.M. McCurry**, None; **S. Sunilkumar**, None; **S.M. Subrahmanian**, None; **E.I. Yerlikaya**, None; **A.L. Toro**, None; **A.M. VanCleave**, None; **S.A. Stevens**, None; **A.J. Barber**, None; **J.M. Sundstrom**, None; **M.D. Dennis**, None

References

1. Lundeen EA, Burke-Conte Z, Rein DB, et al. Prevalence of diabetic retinopathy in the US in 2021. *JAMA Ophthalmol.* 2023;141:747–754.
2. Rübsam A, Parikh S, Fort PE. Role of inflammation in diabetic retinopathy. *Int J Mol Sci.* 2018;19:942.
3. Kowluru RA, Odenbach S. Role of interleukin-1beta in the pathogenesis of diabetic retinopathy. *Br J Ophthalmol.* 2004;88:1343–1347.
4. Vincent JA, Mohr S. Inhibition of caspase-1/interleukin-1beta signaling prevents degeneration of retinal capillaries in diabetes and galactosemia. *Diabetes.* 2007;56:224–230.
5. Thornberry NA, Bull HG, Calaycay JR, et al. A novel heterodimeric cysteine protease is required for interleukin-1 beta processing in monocytes. *Nature.* 1992;356:768–774.
6. Martinon F, Burns K, Tschopp J. The inflammasome: a molecular platform triggering activation of inflammatory caspases and processing of proIL-beta. *Mol Cell.* 2002;10:417–426.
7. Franchi L, Muñoz-Planillo R, Núñez G. Sensing and reacting to microbes through the inflammasomes. *Nat Immunol.* 2012;13:325–332.
8. Swanson KV, Deng M, Ting JP. The NLRP3 inflammasome: molecular activation and regulation to therapeutics. *Nat Rev Immunol.* 2019;19:477–489.
9. Hornung V, Latz E. Critical functions of priming and lysosomal damage for NLRP3 activation. *Eur J Immunol.* 2010;40:620–623.
10. McKee CM, Coll RC. NLRP3 inflammasome priming: a riddle wrapped in a mystery inside an enigma. *J Leukoc Biol.* 2020;108:937–952.
11. Schmacke NA, O'Duill F, Gaidt MM, et al. IKK β primes inflammasome formation by recruiting NLRP3 to the trans-Golgi network. *Immunity.* 2022;55:2271–2284.e2277.
12. Du J, Wang Y, Tu Y, et al. A prodrug of epigallocatechin-3-gallate alleviates high glucose-induced pro-angiogenic factor production by inhibiting the ROS/TXNIP/NLRP3 inflammasome axis in retinal Müller cells. *Exp Eye Res.* 2020;196:108065.
13. Chen W, Zhao M, Zhao S, et al. Activation of the TXNIP/NLRP3 inflammasome pathway contributes to inflammation in diabetic retinopathy: a novel inhibitory effect of minocycline. *Inflamm Res.* 2017;66:157–166.
14. Loukovaara S, Piippo N, Kinnunen K, Hytti M, Kaarniranta K, Kauppinen A. NLRP3 inflammasome activation is associ-

- ated with proliferative diabetic retinopathy. *Acta Ophthalmol.* 2017;95:803–808.
15. Zhang Y, Lv X, Hu Z, et al. Protection of Mcc950 against high-glucose-induced human retinal endothelial cell dysfunction. *Cell Death Dis.* 2017;8:e2941.
 16. Liu Q, Zhang F, Zhang X, et al. Fenofibrate ameliorates diabetic retinopathy by modulating Nrf2 signaling and NLRP3 inflammasome activation. *Mol Cell Biochem.* 2018;445:105–115.
 17. Chaurasia SS, Lim RR, Parikh BH, et al. The NLRP3 inflammasome may contribute to pathologic neovascularization in the advanced stages of diabetic retinopathy. *Sci Rep.* 2018;8:2847.
 18. Ge K, Wang Y, Li P, et al. Down-expression of the NLRP3 inflammasome delays the progression of diabetic retinopathy. *Microvasc Res.* 2022;139:104265.
 19. Zheng L, Howell SJ, Hatala DA, Huang K, Kern TS. Salicylate-based anti-inflammatory drugs inhibit the early lesion of diabetic retinopathy. *Diabetes.* 2007;56:337–345.
 20. Kowluru RA, Koppolu P, Chakrabarti S, Chen S. Diabetes-induced activation of nuclear transcriptional factor in the retina, and its inhibition by antioxidants. *Free Radic Res.* 2003;37:1169–1180.
 21. Kanwar M, Chan PS, Kern TS, Kowluru RA. Oxidative damage in the retinal mitochondria of diabetic mice: possible protection by superoxide dismutase. *Invest Ophthalmol Vis Sci.* 2007;48:3805–3811.
 22. Tuzcu M, Orhan C, Muz OE, Sahin N, Juturu V, Sahin K. Lutein and zeaxanthin isomers modulates lipid metabolism and the inflammatory state of retina in obesity-induced high-fat diet rodent model. *BMC Ophthalmol.* 2017;17:129.
 23. Ding Y, Yuan S, Liu X, et al. Protective effects of astragaloside IV on db/db mice with diabetic retinopathy. *PLoS One.* 2014;9:e112207.
 24. Cogswell JP, Godlevski MM, Wisely GB, et al. NF-kappa B regulates IL-1 beta transcription through a consensus NF-kappa B binding site and a nonconsensus CRE-like site. *J Immunol.* 1994;153:712–723.
 25. Baeuerle PA, Baltimore D. I kappa B: a specific inhibitor of the NF-kappa B transcription factor. *Science.* 1988;242:540–546.
 26. Traenckner EB, Pahl HL, Henkel T, Schmidt KN, Wilk S, Baeuerle PA. Phosphorylation of human I kappa B-alpha on serines 32 and 36 controls I kappa B-alpha proteolysis and NF-kappa B activation in response to diverse stimuli. *EMBO J.* 1995;14:2876–2883.
 27. Sakurai H, Chiba H, Miyoshi H, Sugita T, Toriumi W. I kappa B kinases phosphorylate NF-kappa B p65 subunit on serine 536 in the transactivation domain. *J Biol Chem.* 1999;274:30353–30356.
 28. Sunilkumar S, Toro AL, McCurry CM, et al. Stress response protein REDD1 promotes diabetes-induced retinal inflammation by sustaining canonical NF-kappa B signaling. *J Biol Chem.* 2022;298:102638.
 29. Sunilkumar S, VanCleave AM, McCurry CM, et al. REDD1-dependent GSK3beta dephosphorylation promotes NF-kappa B activation and macrophage infiltration in the retina of diabetic mice. *J Biol Chem.* 2023;299:104991.
 30. Reichenbach A, Bringmann A. Glia of the human retina. *Glia.* 2020;68:768–796.
 31. Coughlin BA, Feenstra DJ, Mohr S. Müller cells and diabetic retinopathy. *Vis Res.* 2017;139:93–100.
 32. Yang S, Qi S, Wang C. The role of retinal Müller cells in diabetic retinopathy and related therapeutic advances. *Front Cell Dev Biol.* 2022;10:1047487.
 33. Miller WP, Toro AL, Sunilkumar S, et al. Müller glial expression of REDD1 is required for retinal neurodegeneration and visual dysfunction in diabetic mice. *Diabetes.* 2022;71:1051–1062.
 34. Brafman A, Mett I, Shafir M, et al. Inhibition of oxygen-induced retinopathy in RTP801-deficient mice. *Invest Ophthalmol Vis Sci.* 2004;45:3796–3805.
 35. Saadane A, Lessieur EM, Du Y, Liu H, Kern TS. Successful induction of diabetes in mice demonstrates no gender difference in development of early diabetic retinopathy. *PLoS One.* 2020;15:e0238727.
 36. Dai W, Miller WP, Toro AL, et al. Deletion of the stress-response protein REDD1 promotes ceramide-induced retinal cell death and JNK activation. *FASEB J.* 2018;32:fj201800413RR.
 37. Miller WP, Sunilkumar S, Giordano JF, Toro AL, Barber AJ, Dennis MD. The stress response protein REDD1 promotes diabetes-induced oxidative stress in the retina by Keap1-independent Nrf2 degradation. *J Biol Chem.* 2020;295:7350–7361.
 38. Miller WP, Mihailescu ML, Yang C, et al. The translational repressor 4E-BP1 contributes to diabetes-induced visual dysfunction. *Invest Ophthalmol Vis Sci.* 2016;57:1327–1337.
 39. Prusky GT, Alam NM, Beekman S, Douglas RM. Rapid quantification of adult and developing mouse spatial vision using a virtual optomotor system. *Invest Ophthalmol Vis Sci.* 2004;45:4611–4616.
 40. Yu P, Zhang X, Liu N, Tang L, Peng C, Chen X. Pyroptosis: mechanisms and diseases. *Signal Transduct Target Ther.* 2021;6:128.
 41. Miller WP, Sha CM, Sunilkumar S, et al. Activation of disulfide redox switch in REDD1 promotes oxidative stress under hyperglycemic conditions. *Diabetes.* 2022;71:2764–2776.
 42. Li W, Liu X, Tu Y, et al. Dysfunctional Nurr1 promotes high glucose-induced Müller cell activation by up-regulating the NF-kappa B/NLRP3 inflammasome axis. *Neuropeptides.* 2020;82:102057.
 43. Ma M, Zhao S, Zhang J, Sun T, Fan Y, Zheng Z. High glucose-induced TRPC6 channel activation decreases glutamate uptake in rat retinal Müller cells. *Front Pharmacol.* 2019;10:1668.
 44. Fort PE, Losiewicz MK, Reiter CE, et al. Differential roles of hyperglycemia and hypoinsulinemia in diabetes induced retinal cell death: evidence for retinal insulin resistance. *PLoS One.* 2011;6:e26498.
 45. Dennis MD, Kimball SR, Fort PE, Jefferson LS. Regulated in development and DNA damage 1 is necessary for hyperglycemia-induced vascular endothelial growth factor expression in the retina of diabetic rodents. *J Biol Chem.* 2015;290:3865–3874.
 46. Ross C, Chan AH, von Pein JB, Maddugoda MP, Boucher D, Schroder K. Inflammatory Caspases: toward a unified model for caspase activation by inflammasomes. *Annu Rev Immunol.* 2022;40:249–269.
 47. Downs KP, Nguyen H, Dorfleutner A, Stehlik C. An overview of the non-canonical inflammasome. *Mol Aspects Med.* 2020;76:100924.
 48. Cheng Q, Pan J, Zhou ZL, et al. Caspase-11/4 and gasdermin D-mediated pyroptosis contributes to podocyte injury in mouse diabetic nephropathy. *Acta Pharmacol Sin.* 2021;42:954–963.
 49. Hoffmeister L, Diekmann M, Brand K, Huber R. GSK3: a kinase balancing promotion and resolution of inflammation. *Cells.* 2020;9:820.
 50. Dennis MD, Coleman CS, Berg A, Jefferson LS, Kimball SR. REDD1 enhances protein phosphatase 2A-mediated dephosphorylation of Akt to repress mTORC1 signaling. *Sci Signal.* 2014;7:ra68.

51. van Weeren PC, de Bruyn KM, de Vries-Smits AM, van Lint J, Burgering BM. Essential role for protein kinase B (PKB) in insulin-induced glycogen synthase kinase 3 inactivation. Characterization of dominant-negative mutant of PKB. *J Biol Chem*. 1998;273:13150–13156.
52. Zhao J, Wang H, Huang Y, et al. Lupus nephritis: glycogen synthase kinase 3 β promotion of renal damage through activation of the NLRP3 inflammasome in lupus-prone mice. *Arthritis Rheumatol*. 2015;67:1036–1044.
53. Wang Y, Meng C, Zhang J, Wu J, Zhao J. Inhibition of GSK-3 β alleviates cerebral ischemia/reperfusion injury in rats by suppressing NLRP3 inflammasome activation through autophagy. *Int Immunopharmacol*. 2019;68:234–241.
54. Wang S, Su X, Xu L, et al. Glycogen synthase kinase-3 β inhibition alleviates activation of the NLRP3 inflammasome in myocardial infarction. *J Mol Cell Cardiol*. 2020;149:82–94.
55. Arumugam S, Qin Y, Liang Z, et al. GSK3 β mediates the spatiotemporal dynamics of NLRP3 inflammasome activation. *Cell Death Differ*. 2022;29:2060–2069.
56. Miller WP, Yang C, Mihailescu ML, et al. Deletion of the Akt/mTORC1 repressor REDD1 prevents visual dysfunction in a rodent model of type 1 diabetes. *Diabetes*. 2018;67:110–119.
57. Dungan CM, Wright DC, Williamson DL. Lack of REDD1 reduces whole body glucose and insulin tolerance, and impairs skeletal muscle insulin signaling. *Biochem Biophys Res Commun*. 2014;453:778–783.
58. Kuo CY, Maran JJ, Jamieson EG, Rupenthal ID, Murphy R, Mugisho OO. Characterization of NLRP3 inflammasome activation in the onset of diabetic retinopathy. *Int J Mol Sci*. 2022;23:14471.
59. Chen H, Zhang X, Liao N, et al. Enhanced expression of NLRP3 inflammasome-related inflammation in diabetic retinopathy. *Invest Ophthalmol Vis Sci*. 2018;59:978–985.